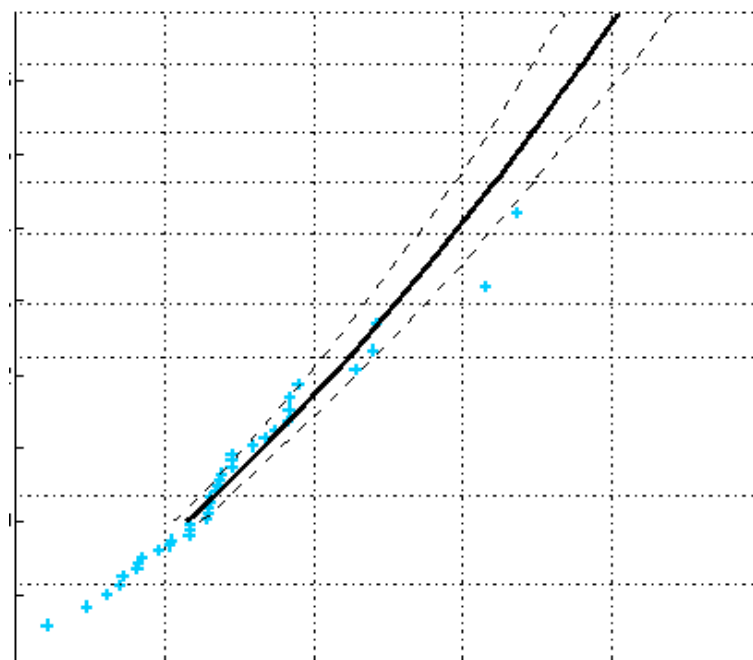


**KJELLER**  
VINDTEKNIKK

## **E39, Bjørnafjorden, Hordaland**

Analysis of extreme wind at the fjord crossing

Report number: KVT/ASH/2018/R089



Report number	Date
<b>KVT/ASH/2018/R089</b>	01.10.2018
Report Title	Availability
<b>E39, Bjørnafjorden, Hordaland</b>	Limited to client
Analysis of extreme wind at the fjord crossing	Revision number
	0
Client	Number of pages
<b>Statens Vegvesen</b>	28 + Appendices
Client Reference	Status
<b>Helle Kristine Fuhr</b>	Final
Summary This report describes the analysis of extreme wind at 10 m height in Bjørnafjorden. Measurements were done during 2015 - 2018, at 4 meteorological masts in Bjørnafjorden, and the models ability to estimate extreme winds is evaluated. The return levels are presented for use in the design basis for the fjord crossing at Bjørnafjorden.	
Disclaimer Although this report, to the best of our knowledge, represents the state-of-the-art in wind energy assessment methods, and efforts have been made to ensure reliable results, Kjeller Vindteknikk AS cannot in any way be held responsible for the use of the findings in the report nor for any direct or indirect losses arising from such use or from errors of any kind in the contents of the report.	

Revision history				
Rev. number	Date	Number of copies	Comment	Distribution
0	2018-10-01	Electronic	Final	pdf

	Name	Digital Signature
Prepared by	Amund S. Haslerud Hálfán Ágústsson Knut Harstveit	
Reviewed by	Rolv Erlend Bredesen	
Approved by	Lars Tallhaug	

# Content

1	Summary.....	3
2	Introduction.....	4
3	Location and topography.....	5
4	Instrumentation and data .....	7
5	Evaluation of measurements and models .....	10
5.1	SYNNØYTANGEN	10
5.2	SVARVHELLEHOLMEN	13
5.3	OSPØYA	14
5.4	SUMMARY OF MODEL-MEASUREMENTS EVALUATION	14
6	Analysis of extreme winds .....	15
6.1	EXTREME WIND ANALYSIS METHODS	15
6.1.1	<i>Generalised extreme value (GEV) method</i> .....	16
6.1.2	<i>Generalised pareto distribution (GP) method</i> .....	16
6.1.3	<i>Gumbel-Lieblein method</i> .....	16
6.2	LONG-TERM ADJUSTMENT USING QUANTILE REGRESSION	17
6.3	CHOICE OF EXTREME VALUE ANALYSIS METHOD	18
6.4	EVALUATION OF EXTREME WIND AT MAST LOCATIONS	21
6.4.1	<i>Vertical profile coefficients at mast locations</i> .....	21
6.4.2	<i>Extreme wind at mast locations</i> .....	22
6.5	RETURN LEVELS AT BRIDGE CROSSING	23
6.6	EXTRAPOLATING UP TO 200 M HEIGHT	25
6.7	SUMMARY OF EXTREME WIND ANALYSIS	26
	References .....	27
	Appendix A - Evaluation of measurements and models .....	i
	Appendix B - Maps of model results .....	vii
	Appendix C - Additional tables .....	ix
	Appendix D - WRF .....	xi

# 1 Summary

In this report, extreme wind around the planned Bjørnafjorden bridge crossing is estimated. A validation of results from the Weather Research and Forecast (WRF) model is carried out, comparing the measurements to model results. The ability to calculate extreme wind is also evaluated, before the extreme winds for selected return periods are estimated.

Return levels of hourly mean winds are estimated at 10 m height for five locations along the crossing, and for six sectors. The locations are south, middle/south, middle, middle/north and north, while the sectors are  $0^{\circ}$ - $75^{\circ}$ ,  $75^{\circ}$ - $225^{\circ}$ ,  $225^{\circ}$ - $255^{\circ}$ ,  $255^{\circ}$ - $285^{\circ}$ ,  $285^{\circ}$ - $345^{\circ}$  and  $345^{\circ}$ - $360^{\circ}$ , in accordance with [1].

The maximum wind speed return levels at 10 m height are listed in Table 1.1 as omnidirectional values. The main focus of this analysis is sector-wise return levels which is presented in Section 6.

Table 1.1: Maximum hourly averaged wind speeds [m/s] along the Bjørnafjorden crossing for given return periods at 10 m height.

Return period	Maximum return level [m/s] at 10 m along fjord crossing
1 year	22.9
10 years	27.1
50 years	30.1
100 years	31.3
500 years	35.5
10,000 years	37.3

In order to be able to estimate return levels between 10 m and 58 m height, a set of profile coefficients are provided. In this way, the presented 10 m return levels are considered best estimates. A second set of profile coefficients are given for estimating the return levels at heights between 58 m and 200 m.

In the special case that one single conservative profile coefficient, independent of sector, is called for, we suggest for convenience one conservative profile coefficient of 0.05 which can be applied on the presented return levels at 58 m to retrieve conservative 10 m values. Similarly, also conservative profile coefficient of 0.14 between 58 m and 200 m are presented (see Table C.1, C.4 and C.5). With the one single conservative profile coefficient of 0.05, the maximum level is increased with 4.3 % compared to Table 1.1 (e.g. the 50 year return value from Table 1.1 increases from 30.1 m/s to 31.4 m/s at the 10 m level).

## 2 Introduction

---

The background for this report is the planned bridge crossing at Bjørnafjorden in Hordaland and the need for an updated description of the climatic conditions in the fjord, pertaining to the design of the crossing.

The report describes the analysis of extreme wind based on measurements from three-dimensional sonic anemometers at 4 meteorological masts in Bjørnafjorden, and from detailed model simulations. The first mast was erected in February 2015 while the last mast became operational in December the same year. The measurements are still ongoing.

Seven bi-annual status reports ([2], [3], [4], [5], [6], [7] and [8]) by Kjeller Vindteknikk describe the observational data and include an analysis of the measured and simulated wind. This includes the short and long-term wind climate, turbulence conditions as well as the spectral statistics of the flow. Observed and simulated extreme winds are analysed and mapped in [9]. The current analysis is based on 2.5 - 3.5 years of observational data, depending on the location. This is a significant increase compared to the previous report and translates to a better description of the long-term climate. However, there is still a limited amount of strong wind events presented in the observational data. A corresponding analysis of even longer time-series is expected to improve the applicability of the extreme winds even further as the coverage of strong wind episodes improve with the duration of the measurement campaign.

### 3 Location and topography

---

Bjørnafjorden (Figure 3-1) is located approximately 30 km south of Bergen and with the communities Tysnes and Austevoll to the south, and Os and Fusa to the north. Bjørnafjorden is roughly 25 km long and has its main axis oriented from west to east at the site of the planned crossing. To the west lies the archipelago of Austevoll and the fjord splits to Langenuen towards south and Korsfjorden and Lysefjorden towards northwest. Eastwards the fjord is relatively open and wide, with ~20 km from the planned crossing towards the easternmost extent of the fjord. The Fusafjorden opens to the northeast, east of the planned crossing.

At the site of the planned crossing, near the masts at Synnøytangen and Svarvhelleholmen, the width of the fjord is on the order of 5 km. Here the terrain is relatively flat, rising to 150 m in the south and 30 m on the northern side. Two masts are located on the small, rocky, island of Ospøya, roughly 5 km west of the planned crossing. An overview map is shown in Figure 3-1 while more details on the locations of the mast and the surrounding topography are found in previous status reports ( [2] - [5]).

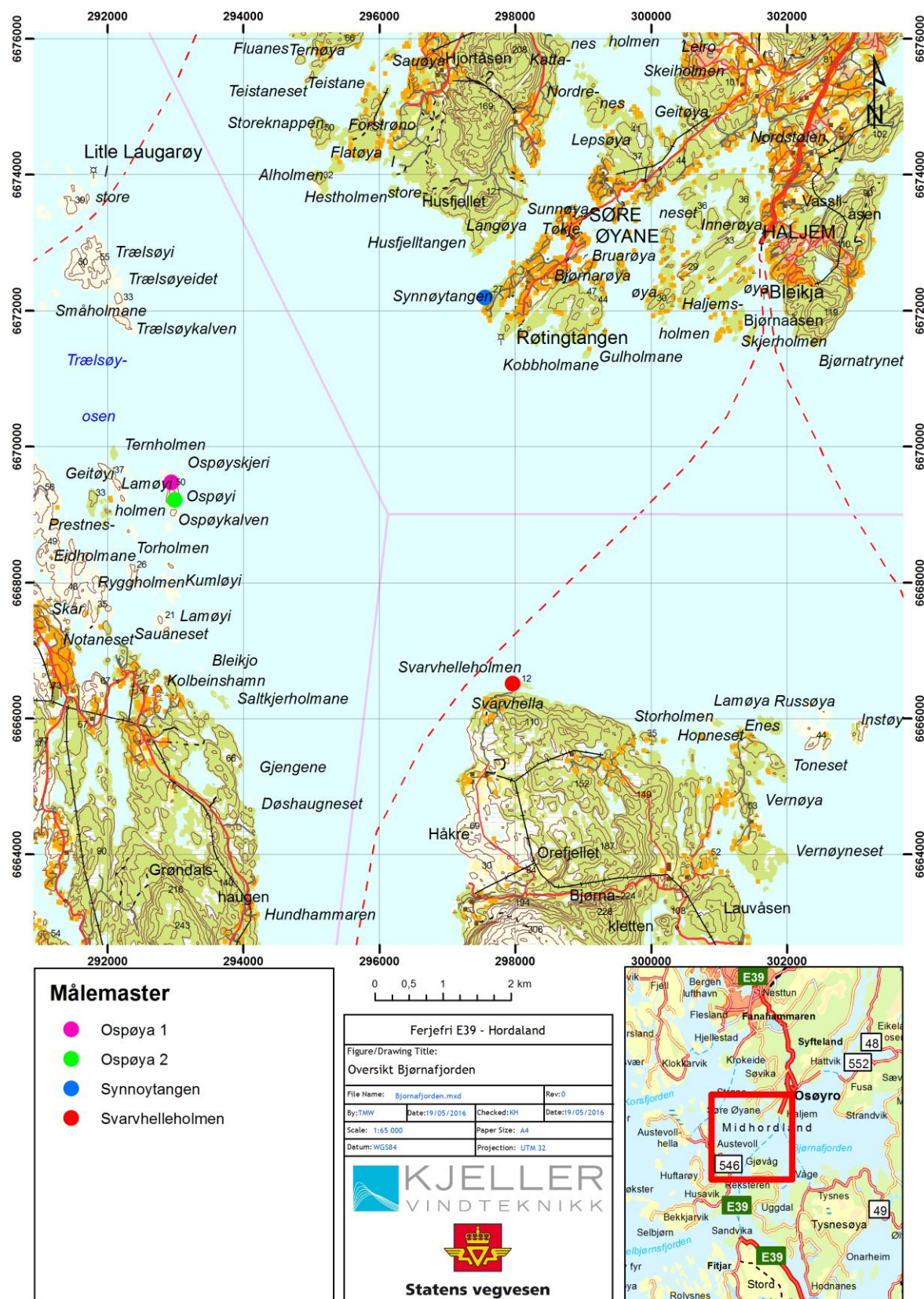


Figure 3-1: Overview of Bjørnafjorden and the masts at Synnøytangen, Svarvhelleholmen, Ospøya 1 and 2.



## 4 Instrumentation and data

The observations are done in tubular masts which are guyed and 50 m high. General information for the mast is summarized in Table 4.1 and Table 4.2, with more details found in [2] - [5].

Table 4.1: General information on the met masts, including observation period.

Mast	Height	Height at base	Coordinates (UTM 32)	Observation period*
Synnøytangen	50 m	26 m	6672190 N, 297558 E	23.02.2015 - 31.05.2018
Svarvhelleholmen	50 m	5 m	6666513 N, 297966 E	18.03.2015 - 31.05.2018
Ospøya 1	50 m	23 m	6669471 N, 292941 E	03.12.2015 - 31.05.2018
Ospøya 2	50 m	34 m	6669215 N, 292989 E	17.12.2015 - 31.05.2018

\* The measurements are on-going. Due to a fault, one sensor on Ospøya 2 became operational at a later date.

The anemometers are placed on horizontal booms (4 m long) at three levels for the masts at Synnøytangen and Svarvhelleholmen (12.7, 31.9 and 48.3 m above ground level). There are also three sensors for both masts on Ospøya. Two sensors are located at 48.8 m a.g.l. on a south-north oriented boom (8 m long), while the third sensor is located at 33.1 m a.g.l. directly below one of the top-sensors. All booms are placed in directions approximately perpendicular to the expected prevailing wind directions.

All measurement instruments are three-dimensional sonic anemometers (Gill WindMaster Pro), and measure the three components of the wind with a sampling frequency of 10 Hz. In 2016, the manufacturer informed about a flaw in the algorithm used in deducing the vertical wind component. The associated error can be corrected by a simple scaling of the observational data. Only corrected data are used here.

Table 4.2: Overview of the instrumentation and nomenclature.

Anemometer	Synnøytangen and Svarvhelleholmen	Ospøya 1* and 2*
	Height [m]	Height [m]
A	48.3	48.8
B	31.9	48.8
C	12.7	33.1

\* Instrument A is 4 m north of the mast while B is 4 m south of mast.

The analysis of spectral coherence is based on filtered and quality controlled 10 Hz datasets from each instrument in the masts. The availability of 10 Hz data is high but there may be sporadic losses which can be traced back to the instruments. These losses cannot be avoided but are typically insignificant. The 10 Hz availability is not reported, but it is well correlated with the availability of data aggregated over a 10-minute interval.



The latest status report [8] includes a report on the data availability of 10-minute averages at the stations in Bjørnafjorden, since start of measurements and until 31 May 2018. The reported availability is reproduced here (Table 4.3), with updates for the data availability for June and July 2018. The availability for 10-minute data is on average high and better than 99 % during most months not associated with major technical problems. The largest problems was due to a lightning strike at Synnøytangen (Nov. - Dec. 2015) and several technical faults (Sep. 2016 - Jan. 2017). A faulty instrument caused a late start of operations for instrument A at Ospøya 2, but the station has also experienced data transmission problems (Oct. 2016). Hence, Table 4.3 reproduces the availability for the B instruments at Synnøytangen and Ospøya 2, not A.

**Table 4.3 Monthly data availability (%) for 10-minute data from the indicated sensors at each of the met masts.**

Synnøyt. B	Jan	Feb	Mar	Apr	May	Jun	Jul	Aug	Sep	Oct	Nov	Dec	Avg.
2015		85.2	99.9	100.0	99.9	99.8	99.9	99.8	100.0	99.8	43.8	46.9	88.6
2016	100	100	100	100	100	100	100	100	91.4	92	100	100	98.6
2017	100	100	100	100	99.2	99.9	100	100	100	100	100	100	99.9
2018	100	100	99.8	100	100	100	100						100
Mean	100.0	96.3	99.9	100.0	99.8	99.9	100.0	99.9	97.1	97.3	81.3	82.3	96.5
Svarvhelleh. A	Jan	Feb	Mar	Apr	May	Jun	Jul	Aug	Sep	Oct	Nov	Dec	Avg.
2015			94.1	99.9	100	100	100	100	100	100	100	100	99.4
2016	98.9	100	100	100	100	100	95.6	99.4	100	100	100	98.8	99.4
2017	97.8	98.8	95.6	100	96.9	99.9	99.4	100	100	100	100	100	99
2018	100	99.7	100	99.9	100	100	100						99.9
Mean	98.9	99.5	97.4	99.9	99.2	100	98.8	99.8	100	100	100	99.6	99.5
Ospøya 1 - A	Jan	Feb	Mar	Apr	May	Jun	Jul	Aug	Sep	Oct	Nov	Dec	Avg.
2015												96.1	96.1
2016	99.6	100	99.7	100	99.5	100	94.9	100	100	100	100	99.5	99.4
2017	98.5	99.6	99.5	100	99.4	99.9	100	100	100	100	100	100	99.7
2018	100	99.7	99.9	99.9	100	100	100						99.9
Mean	99.4	99.8	99.7	100	99.6	100	98.3	100	100	100	100	98.5	99.6
Ospøya 2 - B	Jan	Feb	Mar	Apr	May	Jun	Jul	Aug	Sep	Oct	Nov	Dec	Avg.
2015												100	100
2016	99.3	99.6	100	100	98.9	100	97.9	87.7	100	58.8	95.6	98.8	94.7
2017	98.1	98.9	98.7	99.9	100	99	100	100	100	99.9	99.7	100	99.5
2018	100	98.9	99.9	99.5	100	99.6	99.9						99.7
Mean	99.2	99.1	99.5	99.8	99.6	99.5	99.3	93.8	100	79.4	97.7	99.6	97.6

\*Note that availability during first month is based on the actual start of observations.

## 5 Evaluation of measurements and models

The Weather Research and Forecast (WRF) model has been set up with a horizontal resolution of 500 m x 500 m (denoted WRF500m). Its vertical resolution is 32 levels, where the lowermost levels are at 18 m and 58 m above the surface. The setup is described in Appendix D. Although fine scale, it cannot be expected to reproduce all features of the real topography. Still, an evaluation against the measurement masts is in order.

To evaluate the model against measurements, we use the top-most sensors of the masts.

### 5.1 Synnøytangen

At each hour, the mean wind of the last 10 minutes from the uppermost sensor is evaluated against the closest model data point at the same height and hour. The data series are sorted independently, and are compared in a quantile-quantile plot (QQ-plot). A QQ-plot indicates how well the modelled distribution of wind speeds compare against the measured distribution, but does not take into account the timing of events.

In Figure 5-1, QQ-plots of wind speed for four sectors are shown. The sector is selected from measured data, and does not require the same wind direction for the model. We see that for Synnøytangen, the model compares well for southerly winds, but tends to overestimate northern and eastern winds. For western winds, there is a modest overestimation for winds below 20 m/s. The overestimation from northern and eastern winds is caused by the coarser model topography, making it difficult to capture shielding effects of topography upwind. This may also be the case for westerly modest wind speeds.

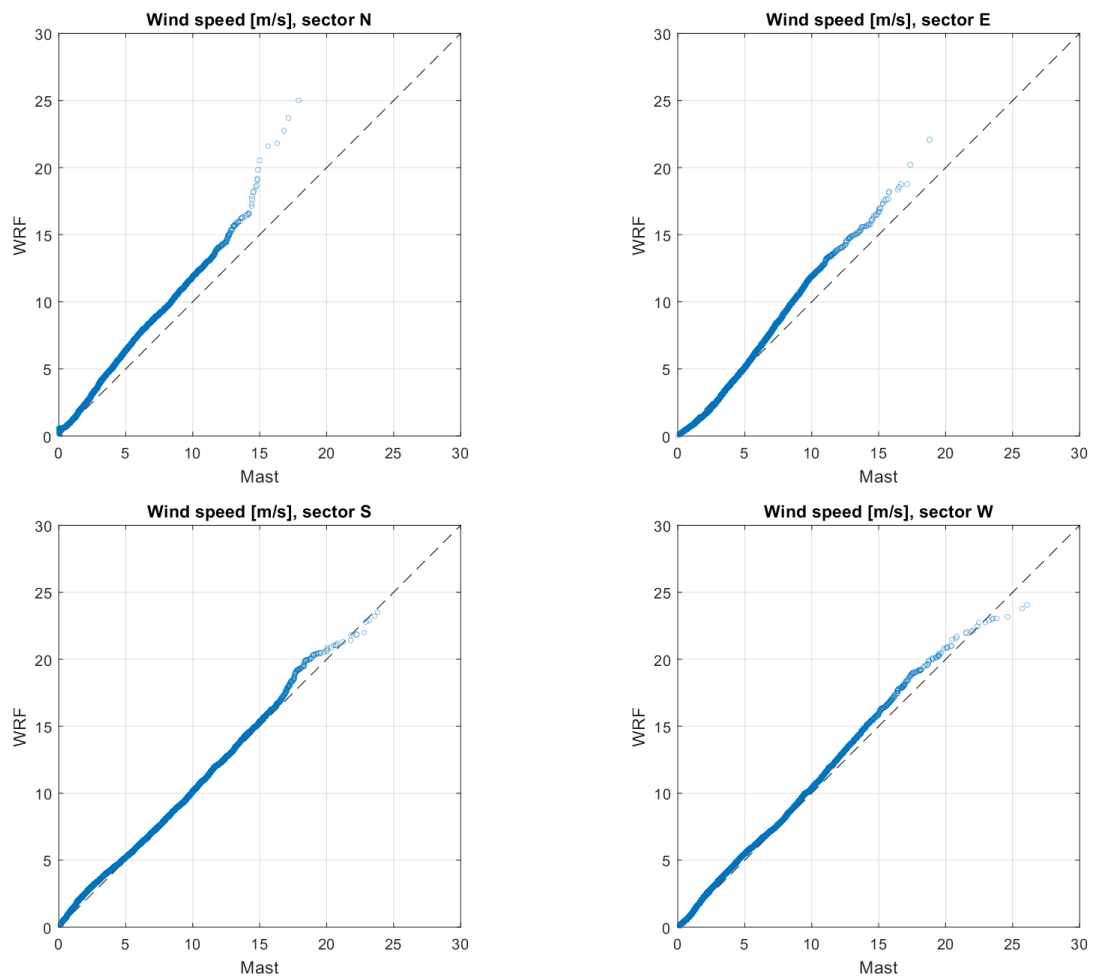
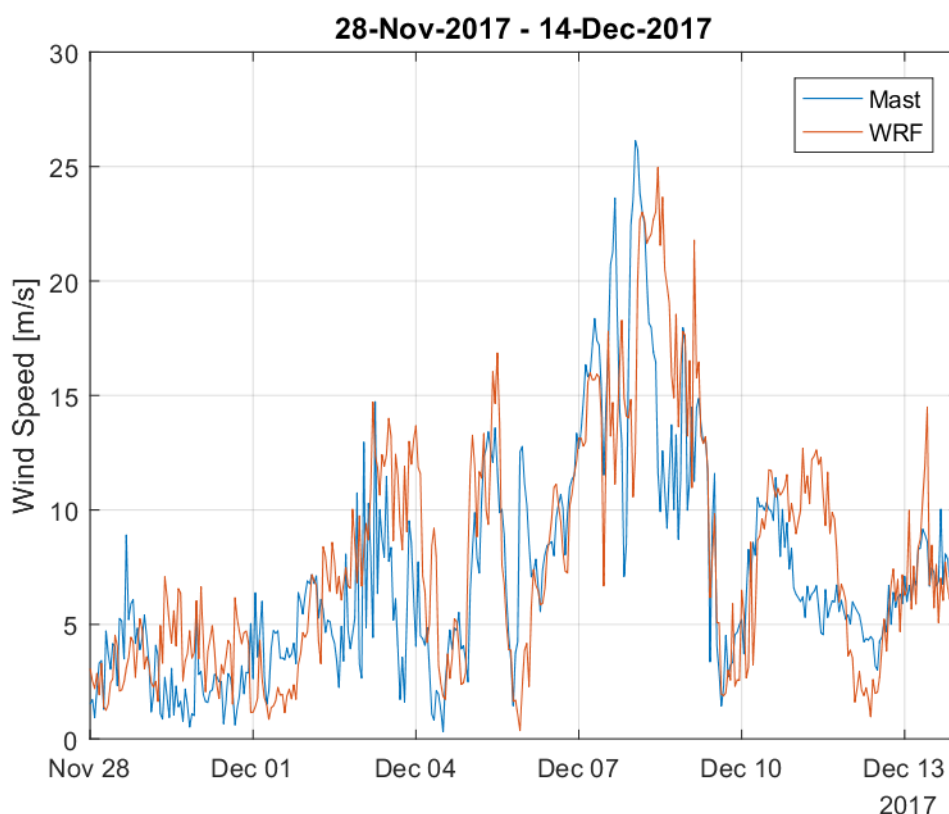


Figure 5-1: QQ-plot of model wind speed against measured wind speed.

It is also important to check whether the strong wind episodes are present in the WRF model simulations. In Figure 5-2 we show measured and modelled wind speed for a period in early December 2017. The strong wind episodes are generally well captured by the model. In Figure 5-3, the corresponding wind direction also shows a good comparison, however with some notable differences: Most pronounced is the differences for northerly winds, which is likely due to the topography not being fully resolved in WRF. For northerly weak winds in the model, the real topography acts to steer the wind in a slightly north-easterly direction. For 11-12 December, WRF predicts wind from the south where measurements show easterly and weaker winds, probably due to topography effects. A typical difficulty in capturing the timing of events can be seen in the shift from north-westerly wind to easterly wind at 4. December, where WRF somewhat lags the measurements.



**Figure 5-2: Comparison of modelled and measured wind speed during a period of strong winds in December 2017.**

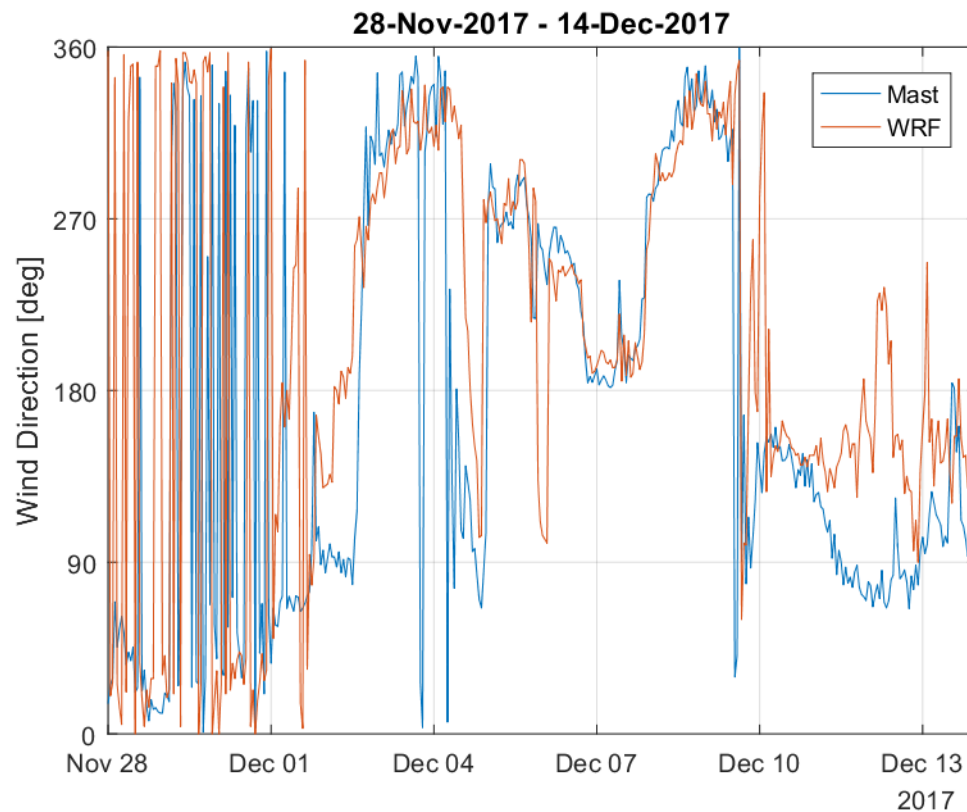


Figure 5-3: Comparison of modelled and measured wind direction during the period of strong winds in December 2017.

Even though there are differences, the model performs well and captures most of the high wind speed events, perhaps slightly underestimated. Wind direction is well captured during high wind speed events.

## 5.2 Svarvhelleholmen

The QQ-plot of Svarvhelleholmen (Figure A-1 in Appendix A) shows similar features as Synnøytangen for sector N and E. For southerly winds, however, the model overestimates substantially, while westerly winds are fairly well reproduced. The southerly overestimation is caused by the model's coarser topography, so that model wind directions are less representative for this sector. This is seen in a QQ-plot of wind direction in Figure 5-4, where the model indicates more southerly winds than in the measurements. The timeseries plots (Figure A-2 and Figure A-3) also confirm this; topography will steer the southerly wind around Reksteren, a feature not captured well in the model. Since the strongest winds are not from the south, the consequences are minor to the extreme value analysis.

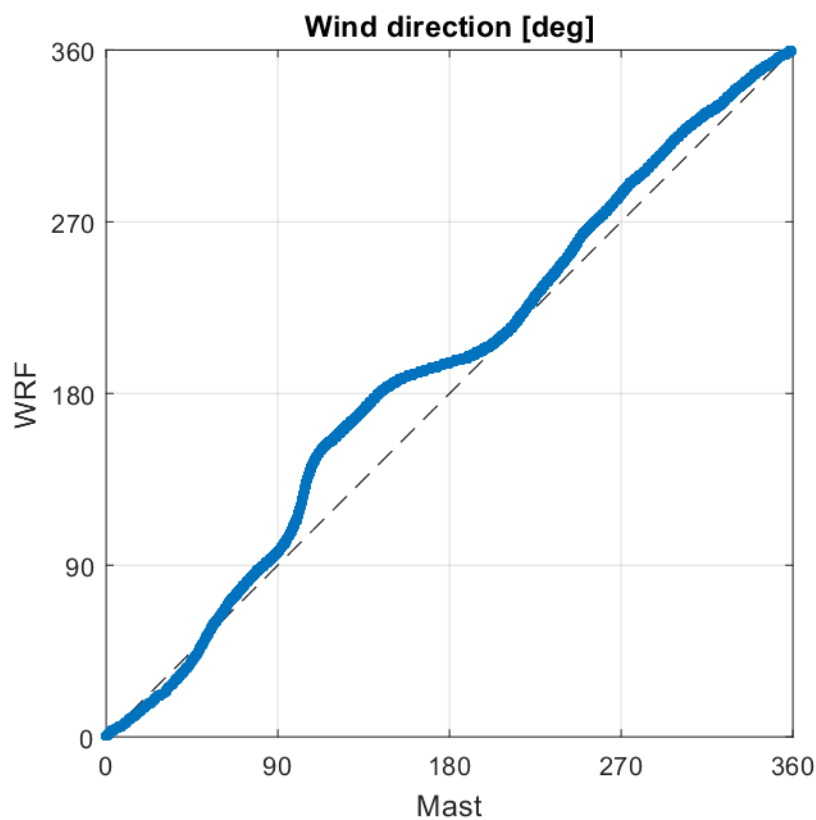


Figure 5-4: Svarvhelleholmen: QQ-plot of wind direction.

### 5.3 Ospøya

The WRF model performs very well at reproducing the top-sensor A measurements Ospøya 1, as shown in Figure A-4. The B sensor and Ospøya 2 shows similar results (not shown). Wind from west is somewhat higher in the model for wind speeds 10-25 m/s, but the overprediction levels off for higher wind speeds. Maximum wind speeds are generally well reproduced (Figures A-5 and A-6).

### 5.4 Summary of model-measurements evaluation

To summarise, the model captures high wind speeds and their directions. The main differences between mast and measurements can be explained by topography being coarsely represented in the model.



## 6 Analysis of extreme winds

When long data series exist, an extreme value distribution using yearly extreme wind speeds can be applied. There are, however, also methods that can be applied to shorter time series, taking more frequent independent maxima into account. In this Section, we will evaluate some extreme value analysis methods, and use the best option in the analysis of extreme wind in Bjørnafjorden.

Depending on application, the extreme wind can be calculated based on maximum 10-minute average wind during each hour, or based on hourly mean winds. Here we will use the former when evaluating the model against measurements, and the latter for the bridge location - as requested by the client. The return levels at the fjord crossing will be estimated for several return periods, and will be presented at 10 m height above the surface.

For the model estimates, the return levels at model level 2 (58 m height) are found and transposed down to 10 m using the modelled sector-wise profile coefficients between model level 2 and 1 (18 m height).

For the evaluation of model against mast measurements, we will estimate return levels at the top sensor height, and also compare modelled and measured profile coefficients.

The sector-wise analysis will be carried out in uneven bins, following the Design Basis of Bjørnafjorden [1] as listed in Table 6.1.

Table 6.1: Sectors used in this analysis [1].

Number	1	2	3	4	5	6
Sector	0°-75°	75°-225°	225°-255°	255°-285°	285°-345°	345°-360°

### 6.1 Extreme wind analysis methods

There are several methods for estimating the extreme winds for given return periods. To analyse extreme winds, it is important to analyse a series of independent maxima. A well-used method is the generalized extreme value (GEV) distribution, which usually takes annual maxima into account. Taking more maxima into account is often done when fitting the generalised pareto distribution (GP) using a peak over threshold (POT) selection of data points. All three methods are applied regularly at Kjeller Vindteknikk.

Generally, when analysing extreme wind, the input to the analysis is hourly values of the maximum 10-minute average wind during the last hour. Model data, however, is given instantaneously each hour, and may be more representative as a 10-minute mean. In previous studies, Kjeller Vindteknikk has found that the model hourly data can be scaled up by 7 % to represent the maximum 10-minute average wind during the last hour.

When comparing to mast measurements, we will apply this factor for model data. However, for the analysis on the bridge location, the focus is hourly mean winds, and the factor will not be applied.

### 6.1.1 Generalised extreme value (GEV) method

The GEV method applied here is provided through the fevd package of the program R. It is a three-parameter model, combining Gumbel [10], Fréchet [11] and Weibull [12] maximum extreme value distributions, with the probability density function:

$$f(x) = \begin{cases} \frac{1}{\sigma} \exp(-(1 + kz)^{-1/k})(1 + kz)^{-1-1/k} & k \neq 0 \\ \frac{1}{\sigma} e^{-z-e^{-z}} & k = 0 \end{cases} \quad \text{Eq.1}$$

$k$ ,  $\sigma$  and  $\mu$  are the shape, scale and location parameters, respectively, and  $z=(x-\mu)/\sigma$ . The GEV method applies by default the maximum likelihood estimation (MLE), although other methods are also available. In this report also the Bayesian approach is applied.

### 6.1.2 Generalised pareto distribution (GP) method

The generalised pareto distribution is described by [13], and applies a peak over threshold (POT) method, where only values above a given threshold are analysed. The reasoning behind the POT method is to study the shape of the tail of the distribution, i.e. the extreme values. Both MLE and Bayesian approaches will be applied here.

### 6.1.3 Gumbel-Lieblein method

A generally accepted method is the Gumbel method [10] with the Lieblein method [14], [15] for optimizing the curve to the observations. Data sets of yearly extremes of the data regardless of direction (omni-sector) are used as input data. The wind year is defined as 1 September to 31 August to ensure independent data from year to year due to the typical stormy season in December/January and the low stormy season during the summer.

The Gumbel distribution, also named the Fisher-Tippet Type I distribution, can be written as

$$P(v > V) = 1 - e^{-e^y} = 1 - e^{-e^{(a_1 V - a_2)}} \quad \text{Eq. 2}$$

where  $a_1$  and  $a_2$  represent the two parameters to be optimized. This is a type of GEV with shape parameter 0. The maximum yearly values of the 1 hour time series were used as input data, and wind speeds of return periods 2 - 100 years were calculated.

The wind speed,  $U$ , is plotted versus  $Y$ , where  $V=U^2$  is used as input parameter to the Gumbel distribution. The corresponding return period and probability of non-exceedance are given on the y-axis. The curve is concave due to the use of  $V=U^2$  as the transformed parameter in the Gumbel-distribution. This is commonly accepted for Rayleigh distributed wind stations (Weibull shape parameter  $k = 2.0$ ).

The Lieblein method is used for fitting the curve to the observed yearly extremes. The method gives less weight to the highest and lowest values, and is therefore less sensitive

to outliers like error values or very seldom storms occurring in the observation series compared to other methods (method of moments, least square or maximum likelihood).

## 6.2 Long-term adjustment using quantile regression

The measured time series are relatively short, and will not cover the range of high wind episodes needed for an extreme value analysis. It is therefore necessary to long-term adjust the data. This is also the case for a short model time series.

Both the measurement and fine resolution model time series are compared to and related to a reference station on hourly basis with a technique called quantile regression. Further information on the methodology can be found in [16] (wherein described as the U&N method). In this analysis a second WRF dataset is used as the primary reference station. This dataset is set up in 4 km x 4 km horizontal resolution (WRF4km), and is available for the period January 1979 through May 2018. The WRF setup is described in Appendix D.

The wind speed and the wind direction are treated separately in the method.

The wind direction adjustment is carried out by first identifying the difference in wind direction between the met mast and the reference station for the prevailing wind direction of the reference station. The concurrent data are then adjusted in accordance with the wind direction difference, and sorted individually in ascending order. The wind direction adjustment to be applied is found by looking at the difference between the sorted datasets using a QQ-approach.

In the wind speed adjustment, the sorted wind directions are divided into 8 sectors in such a way that they all contain the same amount of data. The wind speeds in each of the 8 sectors are sorted individually for the mast and for the reference station to find wind speed adjustment functions. In order to extrapolate velocities outside the range of simultaneous data a regression line is made based on the upper 20 % of the data. This regression line is used as function for extrapolating the 10 % highest velocities captured in the dataset of simultaneous data.

If the simultaneous dataset contains few samples, or any of the datasets contain extreme outliers the extrapolation may create unphysically large wind speeds. To avoid this, the trend line is not used for extrapolation beyond the highest velocity in the simultaneous data; the extrapolation is instead done by following a line of constant ratio, corresponding to the difference of the highest value of the trend line at the highest value in the reference station of the simultaneous data.

This methodology is consistent in the manner that both the distribution of the velocity and the wind direction in the corrected timeseries (or synthesized timeseries) will be equal to the site timeseries in the concurrent period, although the timing can be different. The accuracy of the timing will depend on the correlation between the site and reference station. For extreme wind application of this report the most important aspect is how good the trend line is able to resolve the velocity ratio for the highest wind speeds. The ability to depict the trend line accurately typically improves with the length of the measurement campaign and with the number of storms experienced during the campaign.

To account for higher temporal sampling of the measurements compared to the WRF4km (10-min versus hourly output), the maximum 10-min average during a time window spanning 60 minutes prior to the WRF4km timestamp is used when the met mast is synthesized with the WRF4km dataset.

When the WRF500m time series are synthesized, the hourly values are applied, but when extreme values from model are compared to measured 10-min maxima, a scaling factor is applied.

### 6.3 Choice of extreme value analysis method

The top sensor measurements at Synnøytangen (48.3 m) is long-term adjusted with WRF4km data, and then the extreme value analysis is carried out on the 39 year long dataset (1979-2018).

The GEV and GL methods both take annual maxima into account. Here we apply the GEV using maximum likelihood estimation (MLE) and a Bayesian approach available in the fevd package of R. The GP method, however takes several independent storms into account, but only storms above a user-defined threshold. The choice of threshold value may be problematic. If the threshold is too low, weaker winds will be given a larger weight, and if the threshold is too high, the strongest winds may be given too high weight. It is also possible that the resulting fit is unphysical, giving larger and larger increases in return levels for increasing return periods.

To separate the storms applied in the GP method, we apply a minimum temporal distance of four days between maxima.

The results are shown in Table 6.2, showing that the methods are very similar for return periods up to 10 years, while diverging for longer return periods. Corresponding curve fits are shown in Figure 6-1. It can clearly be seen that the GL method produces a better fit for wind speed in the medium range (26-33 m/s), than GEV and GP with MLE do. As noted in Section 6.1.3, GL also gives lower weight to the low wind speeds. From Figure 6-1, GEV seems to give more weight to the highest wind speeds. Some have pointed out that MLE is less suited for series shorter than 50 data points [17], which is the case for our time series of annual maxima. We have therefore also applied a Bayesian approach in GEV. However, this gives an even higher weight to the highest wind speeds. The shape of the fit is linearly increasing for the highest wind speeds, which is not how extreme wind speeds should behave - return levels should level off with increasing return periods.

The GP with 20 m/s threshold is very similar to the GL method, Bayesian slightly better than MLE, although for a higher threshold of 25 m/s the results are unphysical.

Table 6.2: Hourly 10-minute maximum return levels for selected return periods calculated with different methods for the Synnøytangen top-mast sensor.

Method\return period	2	10	25	50	100
Gumbel-Lieblein	27.2	32.2	34.5	36.0	37.5
GEV(MLE)	27.3	33.2	36.1	38.3	40.6
GEV(Bay.)	27.2	33.0	35.9	38.2	40.4
GP(MLE) (U > 20 m/s)	28.0	31.9	33.9	35.3	36.6
GP(Bay.) (U > 20 m/s)	28.1	32.3	34.5	36.1	37.6

The main draw-back with the GP is the threshold value needed to do the analysis, and the fact that it may alter the shape towards unphysical forms. A too low threshold will reduce the estimated return levels, and for too high thresholds, the curve may bend upwards with increasing return periods, which is unphysical. GEV with Bayesian approach clearly shows potential for errors, and although GEV with MLE seems physically possible, it could be a problematic choice due to few data points. The GL method produces a better fit, and will be used in this work. As already noted, the GL method has the advantage that the highest outliers and the lowest values are given less weight.

Considering the spread of the return values in Table 6.2, the difference between GL and GP is within about 1 m/s up to 100 years return level. Their difference to GEV is about 3-4 m/s for 100 years return level. Based on the results here, GEV is likely too high. Still, the range of results show that there will be some uncertainty to the calculated return levels.

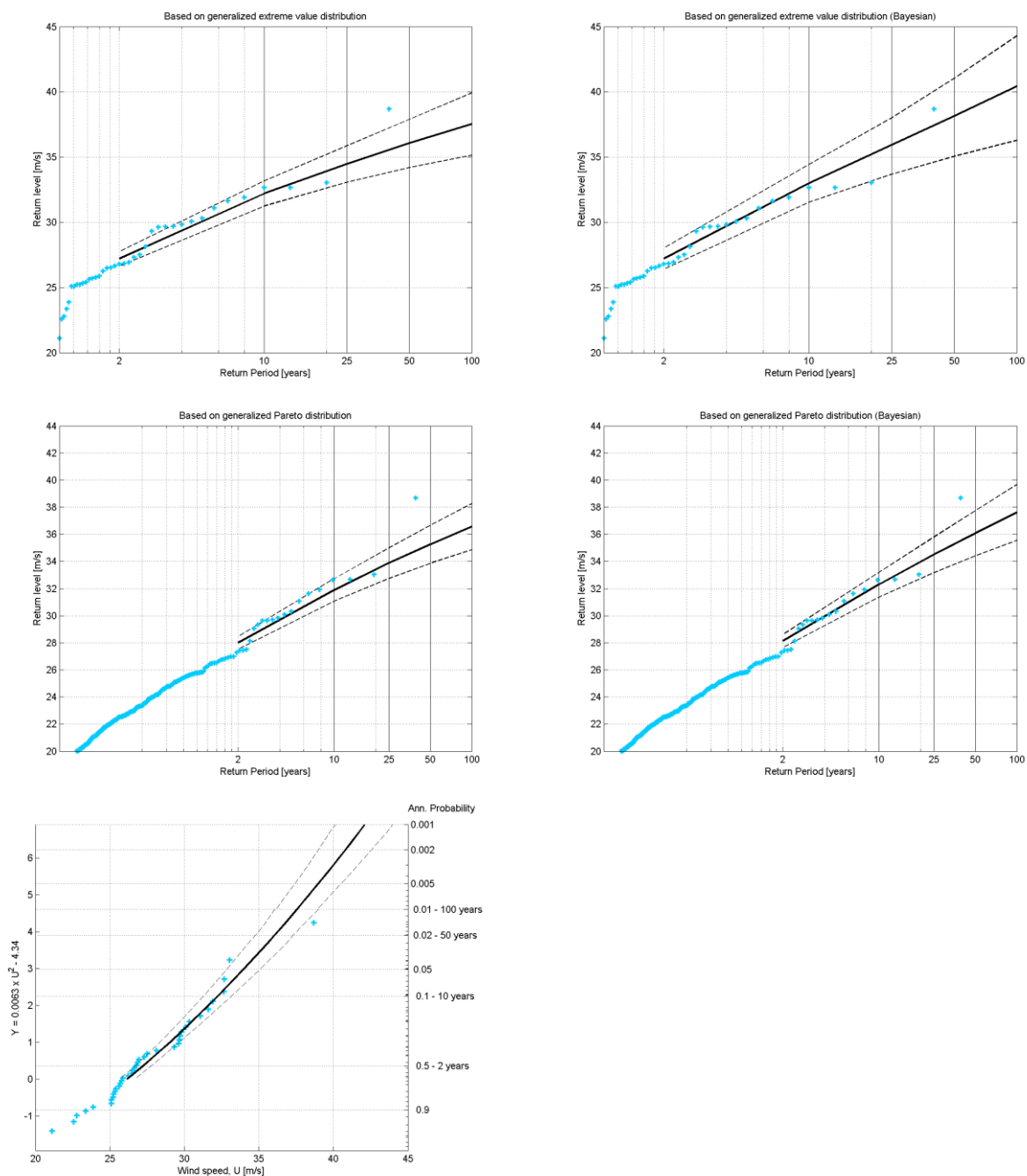


Figure 6-1: Fitting of high speeds events to extreme value distributions, by using the GEV with MLE (top left) and Bayesian approaches (top right), GP with MLE (middle left) and Bayesian approaches (middle right), and the Gumbel-Lieblein method (bottom). Dashed lines show the 68 % confidence interval. Note that wind speed is on the y-axis for GEV and GP, while on the x-axis for GL.

## 6.4 Evaluation of extreme wind at mast locations

In order to use the model data to estimate the extreme wind at the bridge, we compare 50-year return period of hourly maximum of 10-minute averages, for the model and mast. We also compare the vertical profiles.

### 6.4.1 Vertical profile coefficients at mast locations

After long-term adjusting the measured hourly maximum of average 10-minute wind at the mast top sensor (about 48 m height) and the sensor below (about 33 m), we then select the five strongest storms independently for each height and for each of the defined sectors in Table 6.1. These are next averaged for each sector and for the direction-independent storms, and are listed in Table 6.3. It can be seen that for some sectors, the wind is higher at the lower sensor. At Ospøya, Only the A sensors are used since A is the sensor directly above the C sensor below.

Table 6.3: Mean wind speeds for the five strongest storms, calculated from long-term adjusted mast measurements at top sensor and sensor below. Omni means direction-independent.

Mast	Directions						Omni
	0-75	75-225	225-255	255-285	285-345	345-360	
Synnøytangen 48.3m	17.6	31.5	29.9	27.0	31.3	19.8	33.6
Synnøytangen 31.9m	16.8	30.1	28.2	25.3	31.4	18.5	32.9
Svarvhelleholmen 48.3m	18.5	26.2	25.6	26.7	31.9	18.3	32.1
Svarvhelleholmen 31.9m	20.9	24.4	24.1	26.0	30.6	17.1	30.7
Ospøya 1A 48.8m	21.3	29.1	26.8	24.8	31.7	28.3	33.4
Ospøya 1C 33.1m	22.5	28.3	26.0	24.3	31.4	28.1	33.1
Ospøya 2A 48.8m	19.3	30.1	27.8	23.9	32.6	25.9	33.4
Ospøya 2C 33.1m	22.1	28.6	27.5	24.7	32.4	26.6	33.8

For extreme wind conditions, the profile coefficient  $\alpha$  between two levels is found using the wind profile power law

$$\frac{U_2}{U_1} = \left(\frac{z_2}{z_1}\right)^\alpha$$

giving the profile coefficient

$$\alpha = \frac{\log \frac{U_2}{U_1}}{\log \frac{z_2}{z_1}}$$

where  $U_2$  is the average wind speed of the five strongest storms at the height  $z_2$ , and  $U_1$  is the average wind speed of the five strongest storms at the height  $z_1$ . For the model results, the model levels at 58 m and 18 m height are used.

In Table 6.4 and Table 6.5 we present the profile coefficients calculated from measurements and from model, respectively. For direction  $0^\circ$ - $75^\circ$ , all masts except Synnøytangen show stronger winds closer to the ground than higher up (negative profile



coefficient). Synnøytangen shows a similar effect for the 285°-345° sector, with stronger winds closer to the ground, caused by the topography at the location. For Ospøya 2 (the southern mast), speed-up effects can also be seen for winds from the 255°-285° sector, which is not seen for Ospøya 1, and from sector 345°-360°. Ospøya 2 shows speed-up closer to the ground also for the direction independent high winds, but for sector 75°-225° there seems to be very little speed-up. These features can be explained by the topography of Ospøya. It should be noted that Ospøya 2A has a shorter measurement period, which possibly could explain some of the differences to 1A.

The model does not capture the speed-up effects well, giving only positive profile coefficients. This is to be expected, since finer topography details are not resolved. However, the profile coefficients match quite well where no obvious speed-up should be present, exemplified by Svarvhelleholmen for sector 285°-345°, and by most sites for sector 75°-225°. The local speed-up effects at mast sites are less relevant for the bridge crossing some distance from land; the mast measurements cannot be used to derive profile coefficients in the open fjord. However, when using the model to estimate of the 10 m extreme wind across the fjord, care should be taken close to land.

Table 6.4: Profile coefficients calculated from mast measurements at top sensor and sensor below.

Mast	Directions						Omni
	0-75	75-225	225-255	255-285	285-345	345-360	
Synnøytangen	0.121	0.110	0.143	0.158	-0.005	0.154	0.051
Svarvhelleholmen	-0.293	0.171	0.139	0.059	0.105	0.164	0.106
Ospøya 1A	-0.137	0.078	0.082	0.055	0.023	0.015	0.021
Ospøya 2A	-0.342	0.131	0.027	-0.086	0.017	-0.069	-0.030

Table 6.5: Profile coefficients calculated from the model levels at 58 m and 18 m, at mast positions. For Ospøya only one set of profile coefficients are given, since the data point used is the same for Ospøya 1 and 2.

Closest model grid point	Directions						Omni
	0-75	75-225	225-255	255-285	285-345	345-360	
Synnøytangen	0.207	0.111	0.101	0.099	0.108	0.142	0.104
Svarvhelleholmen	0.112	0.152	0.133	0.102	0.090	0.093	0.102
Ospøya 1/2	0.077	0.111	0.141	0.130	0.087	0.088	0.093

#### 6.4.2 Extreme wind at mast locations

As described in Section 6.3, we apply the Gumbel-Lieblein method to estimate return levels for given return periods. From the long-term adjusted time series, the annual maximum storms are found, using winter years (1 September to 31 August). 50-year return levels for measured and model annual maxima are listed in Table 6.6 and Table 6.7, respectively, along with sector-wise return levels. While sector-wise return levels could be estimated by analysing only maxima from each sector, it is not recommended; even a 39

year long time series may not have representative number of storms in all sectors. Instead, the sector-wise return levels are found using the ratio between the average of the five strongest storms in each sector and the average of the five overall strongest storms.

The model-measurement agreement is very good, although the model overestimates slightly for directions where the observed profile coefficient is low, e.g. at Ospøya.

Table 6.6: 50-year return levels calculated from long-term adjusted mast measurements at top sensor.

Mast	Directions						Omni
	0-75	75-225	225-255	255-285	285-345	345-360	
Synnøytangen	18.7	33.5	31.8	28.7	33.2	20.9	35.7
Svarvhelleholmen	19.3	27.3	26.6	27.8	33.3	19.0	33.9
Ospøya 1A	22.3	30.5	28.1	26.0	33.2	29.7	35.0
Ospøya 1B	22.3	30.8	27.7	26.2	34.5	28.6	35.7
Ospøya 2A	20.8	32.4	30.0	25.8	35.1	27.9	36.0
Ospøya 2B	19.9	30.3	27.4	24.9	34.3	27.7	35.6

Table 6.7: 50-year return levels calculated from long-term adjusted model results. Return levels at 58 m model level are transferred to top sensor height by using model profile coefficients in Table 6.5. For Ospøya only one set of results is given, since the data point used is the same for Ospøya 1 and 2.

Mast	Directions						Omni
	0-75	75-225	225-255	255-285	285-345	345-360	
Synnøytangen	19.8	29.5	31.6	32.3	33.0	19.4	34.9
Svarvhelleholmen	20.6	29.6	30.2	28.5	35.1	21.2	35.5
Ospøya 1/2	22.8	32.1	31.6	30.9	36.9	27.2	37.5

## 6.5 Return levels at bridge crossing

Using the modelled profile coefficients and the return levels at the 58 m model level, the return levels at 10 m height can be estimated. These return levels  $U_{10m}$  at height 10 m may then be transferred to another height  $z$  by using the profile coefficient  $\alpha$ :

$$U(z) = U_r \left( \frac{z}{10 \text{ m}} \right)^\alpha$$

The most accurate estimates of the return levels at 10 m can be found using specific profile coefficients for each sector and location. However, such an approach makes a vertical extrapolation a bit tedious, since all values are specific to site and sector.

One alternative approach is to estimate a conservative profile coefficient, and then estimate more conservative return levels at 10 m. Compared to the more detailed approach, this gives higher return levels at 10 m, but is easier to use for extrapolation since only one coefficient would be needed. The two methods would produce the same return levels at 58 m.

In order to avoid an overly conservative analysis, we have estimated profile coefficients at five locations along the bridge, for each sector. The five locations are south, south/middle, middle, north/middle and north. Using these profile coefficients, we estimate corresponding return levels at 10 m. This means that specific return levels and profile coefficients must be applied in an extrapolation, with a total number of points reduced to five locations along the bridge.

All WRF500m profile coefficients for a  $\pm 1$  km span along the bridge are analysed for all sectors. For each of the five locations along the bridge, the median of the closest data points is chosen as profile coefficient, listed in Table 6.8. By selecting the median as the most likely value we avoid building in too much conservativeness in the profile coefficient. If, however, one single conservative profile coefficient is wanted, it should be the lowest value seen for all sectors and points in Table 6.8, which is 0.05. This value gives the least reduction in wind speed when going from 58 m to 10 m, and is conservative for all points except the northeast point and sector 0-75.

Detailed maps of the sector-wise WRF500m profile coefficients are shown in Appendix A, and an overview of model data points analysed is shown at the end of Appendix D.

**Table 6.8: Model profile coefficients along the bridge, calculated from the five strongest storms at 18 m and 58 m height.**

Position	0-75	75-225	225-255	255-285	285-345	345-360
North	0.05	0.10	0.10	0.10	0.10	0.20
North/middle	0.07	0.07	0.13	0.10	0.08	0.13
Middle	0.09	0.06	0.12	0.12	0.08	0.08
South/Middle	0.10	0.10	0.13	0.12	0.07	0.11
South	0.10	0.11	0.13	0.12	0.08	0.11

For the 58 m WRF500m return levels of hourly mean wind, we select the maximum value instead of median. For all points and sectors we find an almost constant ratio between return levels for different return periods. Instead of giving a table for each return period, we show the 50-year return levels in Table 6.9 and present scaling factors for return periods 1, 10, 100, 500 and 10000 years, confirming to the scaling factors of the previous report [9]. In Appendix C we also show the return levels for hourly maxima of 10-minute averages.

The Gumbel-Lieblein method is not designed for estimating the 500 and 10,000 years return levels. Such return levels will be rather uncertain, and are usually found by scaling up either the 50-year or 100-year return levels. For 500-year return level, we apply the scaling factor 1.18 given in NEK 445:2009 [18]. For 10,000-year return level, we apply the average scaling factor based on work at KNMI [19], which is 1.24. As expected, the 10,000-year return level is very uncertain, and other scaling factors may exist.

**Table 6.9: 50-year return levels for hourly mean wind [m/s] at 10 m on bridge, estimated using the profile coefficients in Table 6.8.**

Position	Wind direction						Max
	0-75	75-225	225-255	255-285	285-345	345-360	
North	19.2	21.1	23.9	24.0	24.2	13.7	24.2
North/middle	17.8	25.0	24.8	26.0	28.5	16.8	28.5
Middle	15.7	26.3	25.3	25.3	29.1	18.7	29.1
South/Middle	16.0	25.4	25.0	25.2	30.1	18.8	30.1
South	17.4	24.3	24.4	24.2	29.8	18.1	29.8

**Table 6.10: Scaling factors to convert 50-year return levels in Table 6.9 to other return periods.**

Return period	Scaling factor against 50-year return level	Reference
1 year	0.76	This work
10 years	0.90	This work
100 years	1.04	This work
500 years	1.18	[18]
10,000 years	1.24	[19]

The profile coefficients in Table 6.8 and 10 m return levels in Table 6.9 can only be extrapolated up to 58 m. As background information, the WRF500m estimated 50-year return levels at 58 m are listed in Appendix C, Table C-1. How to extrapolate further up is described in Section 6.6.

## 6.6 Extrapolating up to 200 m height

To be able to extrapolate up from 58 m, we have estimated the profile coefficients between the model levels at 58 m and 193 m, following the same procedure as in Section 6.5. For sectors 225°-255°, 255°-285° and 285°-345°, the profile coefficients are rather similar to the near-surface profile coefficients listed in Table 6.8. These sectors will have fairly similar return values at 193 m. Sector 75°-225°, however, has a higher profile coefficient between 58 m and 193 m than between 18 m and 58 m, resulting in return levels close to the levels of sectors 225°-345° at 193 m height. For the north-northeast sector, there is a notable increase in profile coefficients. However, the return levels will still be notably lower at 193 m than for the other sectors. Finally, for the north-northwest sector the profile coefficients are only slightly increased, and will still be a sector with lower return levels at 193 m.

If one single conservative profile coefficient should be applied when extrapolating above 58 m, it would be 0.14 to account for the increases in the sectors with the highest return levels.

Table 6.11: Model profile coefficients along the bridge, calculated from the five strongest storms at 58 m and 193 m height.

Position	0-75	75-225	225-255	255-285	285-345	345-360
North	0.14	0.16	0.13	0.12	0.12	0.24
North/middle	0.17	0.16	0.13	0.11	0.10	0.22
Middle	0.18	0.15	0.13	0.10	0.09	0.21
South/Middle	0.16	0.12	0.14	0.10	0.08	0.18
South	0.12	0.15	0.15	0.12	0.08	0.16

## 6.7 Summary of extreme wind analysis

Return levels at 10 m height, for five locations on the Bjørnafjorden crossing, are given for six sectors. Corresponding profile coefficients are also listed; one for extrapolation up to 58 m and one for further extrapolation to 200 m. The data needed are Table 6.8, Table 6.9, Table 6.10 and Table 6.11.

Applying one profile coefficient would imply conservative return levels near 10 m. It is possible to derive these return levels from the 58 m return levels in Table C-1. If so, the conservative profile coefficient should be 0.05, and the corresponding conservative return levels at 10 m are listed in Table C-4. Similarly, for extrapolating between 58 m and 200 m, the conservative profile coefficient should be 0.14.

## References

- [1] S. Vegvesen, "Design basis MetOcean," *SBJ-01-C3-SVV-01-BA-001*, 2017.
- [2] T. Willig og K. Harstveit, «E39, brukrysnings Hordaland. Statusrapport for vindmålinger pr juni 2015. KVT/KH/2015/R066,» Kjeller Vindteknikk, 2015.
- [3] K. Harstveit og H. Ágústsson, «E39. brukrysnings Møre og Romsdal. Statusrapport for vindmålinger pr november 2015. KVT/KH/2015/R107,» Kjeller Vindteknikk, 2016.
- [4] T. Willig, «E39, brukrysnings Hordaland. Statusrapport for vindmålinger pr mai 2016. KVT/KH/2016/R041,» Kjeller Vindteknikk, 2016.
- [5] K. Harstveit, H. Ágústsson og T. P. Miinalainen, «E39, brukrysnings Hordaland. Statusrapport for vindmålinger pr november 2016. KVT/KH/2016/R092,» Kjeller Vindteknikk, 2016.
- [6] H. Ágústsson, «E39, brukrysnings Hordaland. Statusrapport for vindmålinger pr august 2017. KVT/HÁ/2017/R083,» Kjeller Vindteknikk, 2017.
- [7] H. Ágústsson, "E39, brukrysnings Hordaland. Statusrapport for vindmålinger pr desember 2017. KVT/HÁ/2018/R007," Kjeller Vindteknikk, 2018.
- [8] H. Ágústsson og F. F. Liland, «E39, brukrysnings Hordaland. Statusrapport for vindmålinger pr mai 2018. KVT/HÁ/2018/R052,» Kjeller Vindteknikk, 2018.
- [9] K. Harstveit, H. Ágústsson og R. E. Bredesen, «Bjørnafjorden, Hordaland. Kartlegging av vindforhold. KVT/KH/2016/R020,» Kjeller Vindteknikk, 2016.
- [10] E. Gumbel, "Statistics of extremes," *Columbia University Press, New York, N.Y.*, 1958.
- [11] M. Fréchet, "Sur la loi de probabilité de l'écart maximum," *Ann. Soc. Polon. Math.* 6, 1927.
- [12] W. Weibull, "A statistical distribution function of wide applicability," *J. Appl. Mech.-Trans. ASME* 18(3), pp. 293-297, 1951.
- [13] S. Coles, "An introduction to statistical modeling of extreme values," Springer, 2001.
- [14] R. Harris, "Gumbel re-visited - a new look at extreme value statistics applied to wind speeds," *Journal of Industrial Aerodynamics*, 59, pp. 1-22, 1996.
- [15] J. Lieblein, "Efficient Methods of Extreme-Value Methodology," *National Bureau of Standards, NBSIR 74-602, Washington*, 1974.
- [16] S. Lileo, E. Berge, O. Undheim, R. Klinkert och R. E. Bredesen, ""Long-term correction of wind measurements. State-of-the-art, guidelines and future work.," *Elforsk report* 13:18, 2013.
- [17] S. Coles och M. Dixon, "Likelihood-based inference for extreme value models," *Extremes*, pp. 2, 5-23, 1999.
- [18] N. E. komite, NEK445:2009: Luftledninger over 1 kV, Norsk Elektroteknisk komite, 2009.
- [19] A. Smits, "Estimation of extreme return levels of wind speed: a modification of the Rijksoort-Weibull model," *KNMI, WM/KD*, 2001.
- [20] KVT/KH/2016/R032, "Sulafjorden, Møre og Romsdal: Analyse av modellert vind, strøm og bølger," Kjeller Vindteknikk, 2016.
- [21] G. Taylor, "The spectrum of turbulence," *Proc. R. Soc. London Ser. A*, vol. 164, pp. 476-490, 1938.

- [22] Statens Vegvesen, Bruprosjektering. Håndbok 400, Oslo, 2015.
- [23] H. Panofsky och J. Dutton, Atmospheric Turbulence. Models and Methods for Engineering Applications., US: John Wiley & Sons, 1984.
- [24] G. Jenkins och D. Watts, Spectral analysis and its applications, San Francisco, US: Holden - Day, 1968.
- [25] L. MacLaren och S. Hill, "A Fortran Program for Spectral Analyzing using the Fast Fourier Transform.," Flight Mechanics Technical Memorandum 432, Department of Defence, Australia, 1991.
- [26] J. Mann, K. L. och N. O. Jensen, "Uncertainties of extreme winds, spectra and coherences. Bridge Aerodynamics," i *Bridge Aerodynamics*, eds Larsen and Esdahl, Rotterdam, Netherlands, Balkema Publishers, A.A. / Taylor & Francis, 199, pp. p. 49-56.
- [27] F. Haan, "The Effects of Turbulence on the Aerodynamic of Long-Span Bridges," Dissertation, University of Notre Dame, Indiana, USA, 2000.
- [28] A. G. Davenport, "The Spectrum of Horizontal Gustiness near the Ground in High Winds," *Q. J. R. Meteorol. Soc.*, vol. 87, pp. 194-211, 1961.
- [29] J. Lindvall, "Kvitneset, E39, Sulafjorden, Møre og Romsdal county: Status report 1," KVT/JL/2017/R038, 2017.
- [30] K. Harstveit og H. Ágústsson, «E39, brukrysninger Hordaland, Ospøya - koherensanalyse, KVT/KH/2017/R023-rev1,» Kjeller Vindteknikk, 2017.



# Appendix A - Evaluation of measurements and models

Here we present additional figures for the main text.

## Svarvhelleholmen

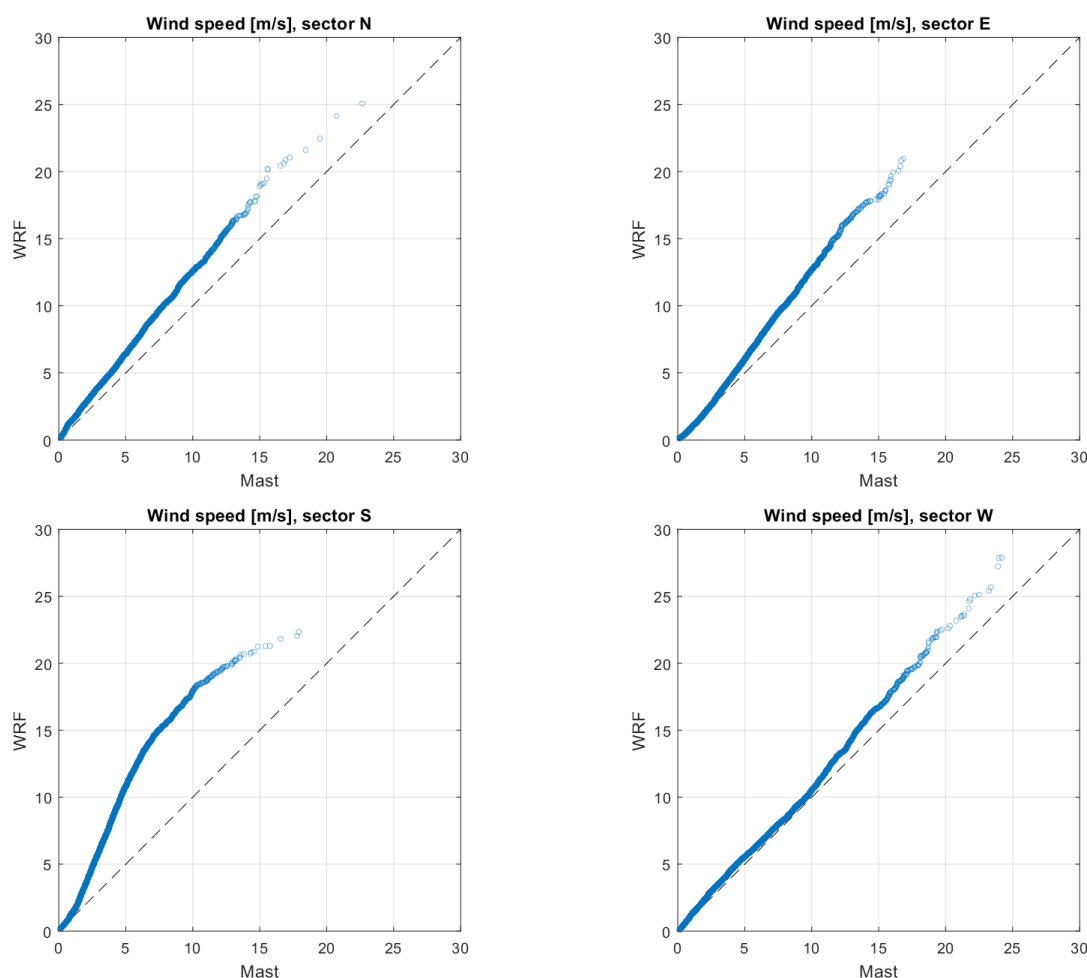
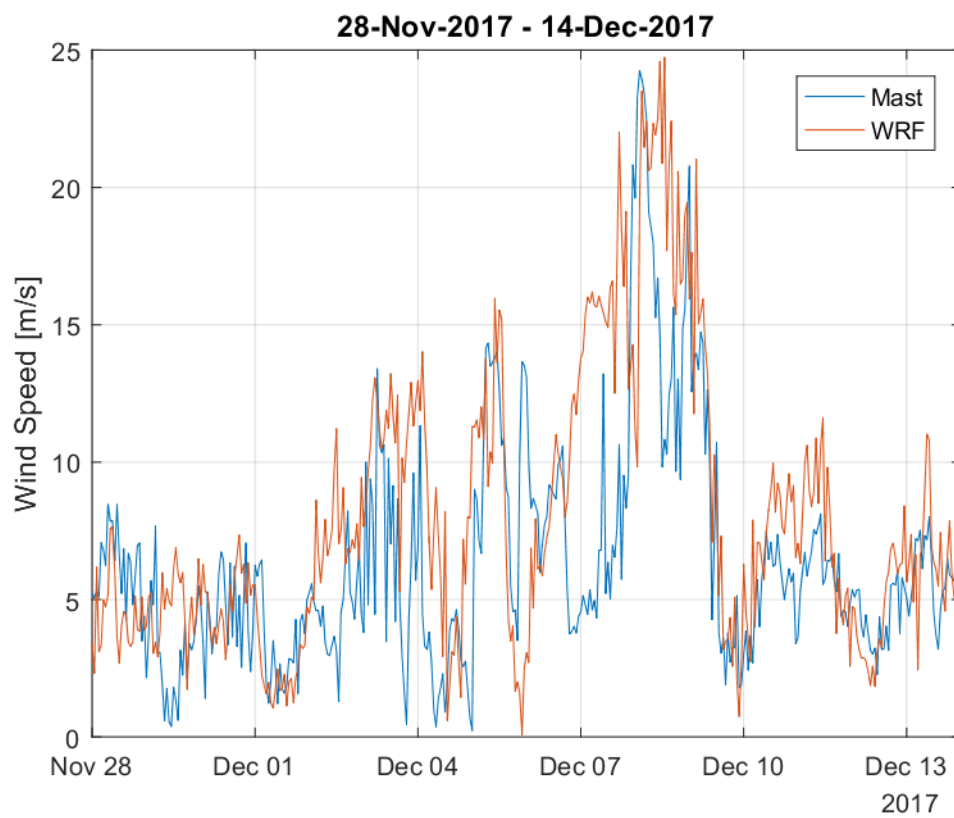
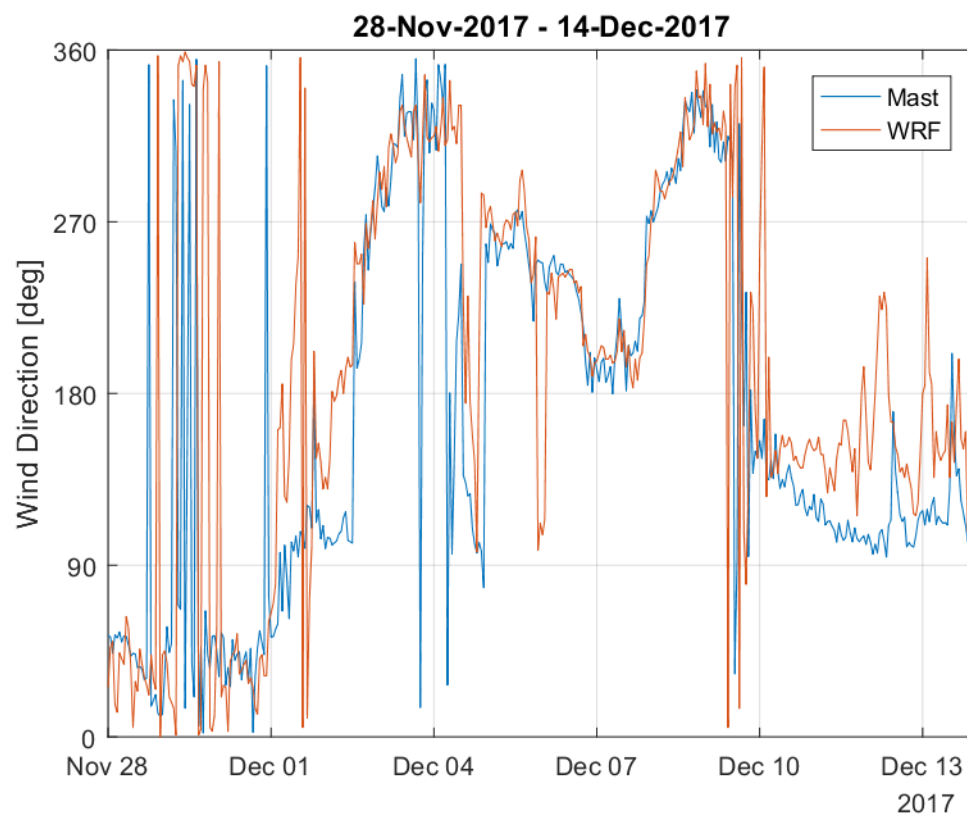


Figure A-1: Svarvhelleholmen: QQ-plot of model wind speed against measured wind speed.



**Figure A-2: Svarvhelleholmen: Comparison of modelled and measured wind speed during a period of strong winds in December 2017.**



**Figure A-3: Svarvhelleholmen: Comparison of modelled and measured wind direction during the period of strong winds in December 2017.**

## Ospøya

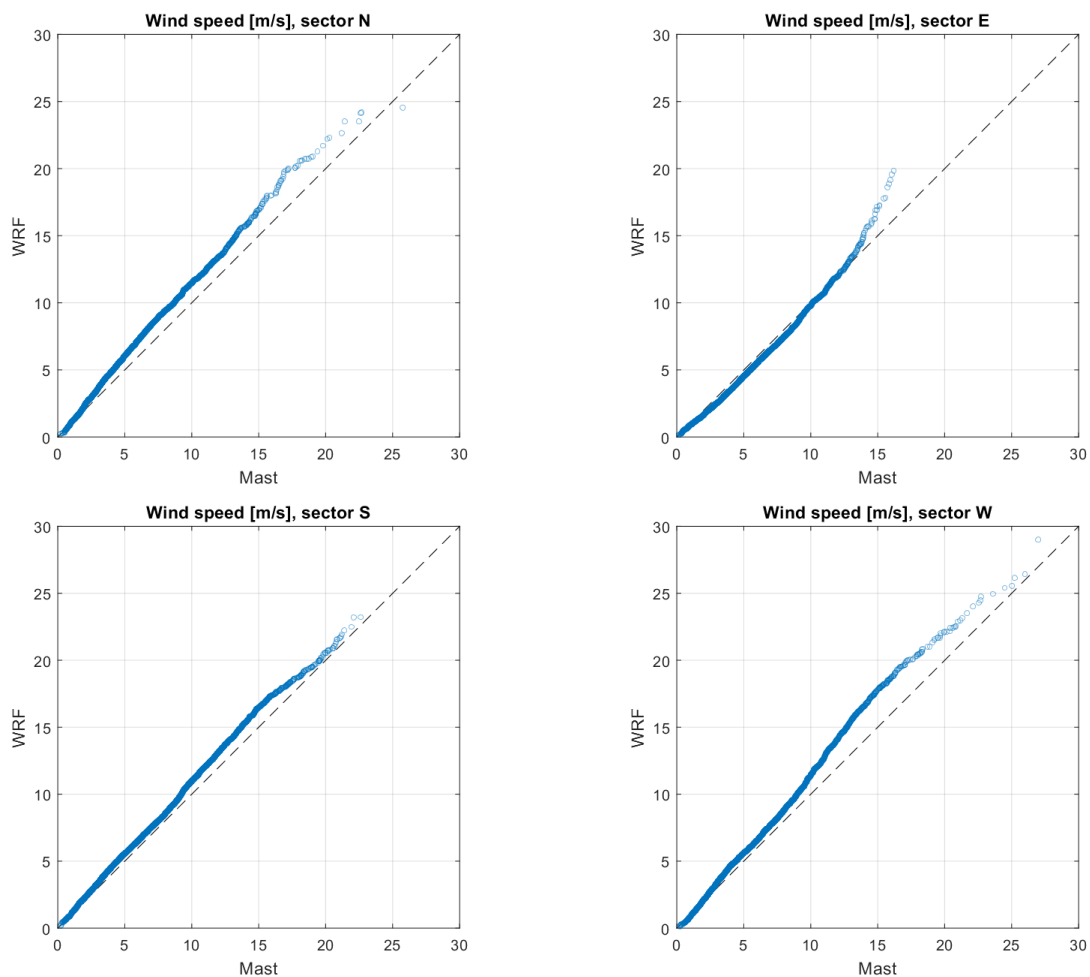
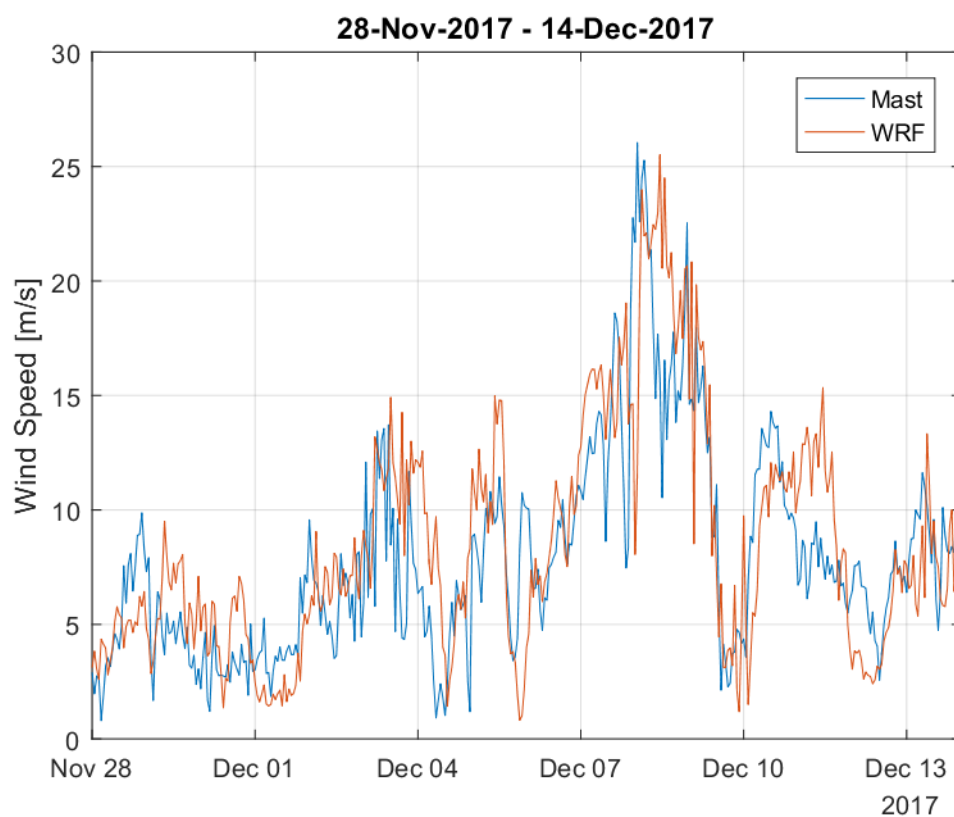
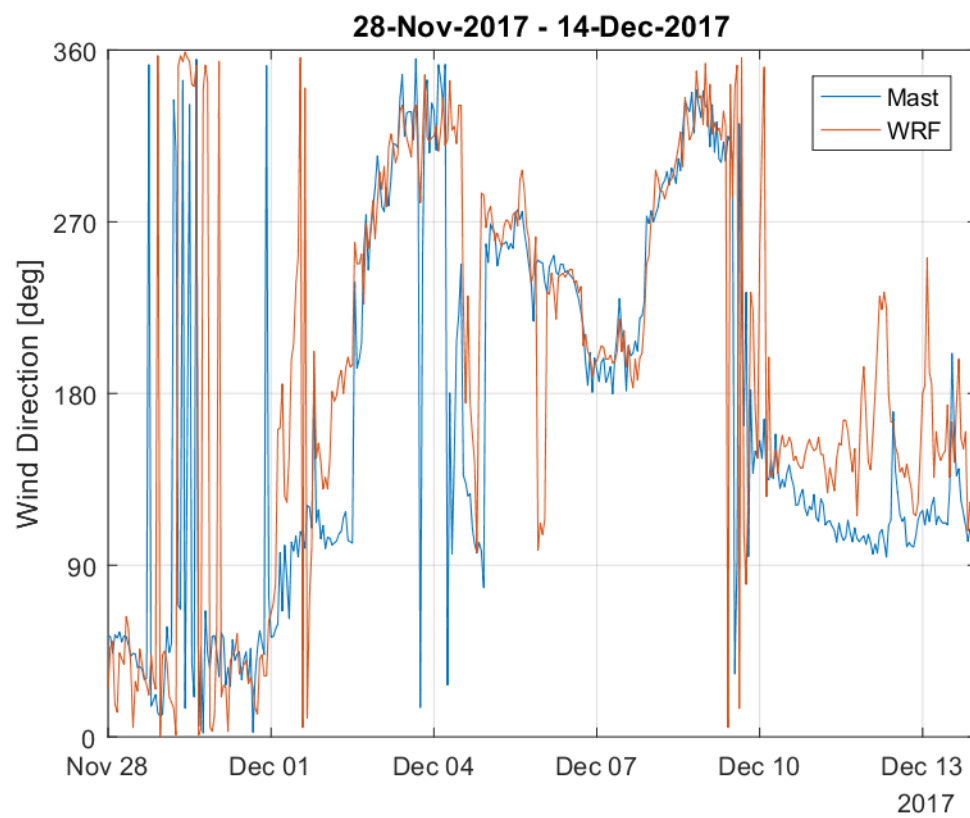


Figure A-4: Ospøya 1A: QQ-plot of model wind speed against measured wind speed.



**Figure A-5: Ospøya 1A: Comparison of modelled and measured wind speed during a period of strong winds in December 2017.**



**Figure A-6: Ospøya 1A: Comparison of modelled and measured wind direction during the period of strong winds in December 2017.**

## Appendix B - Maps of model results

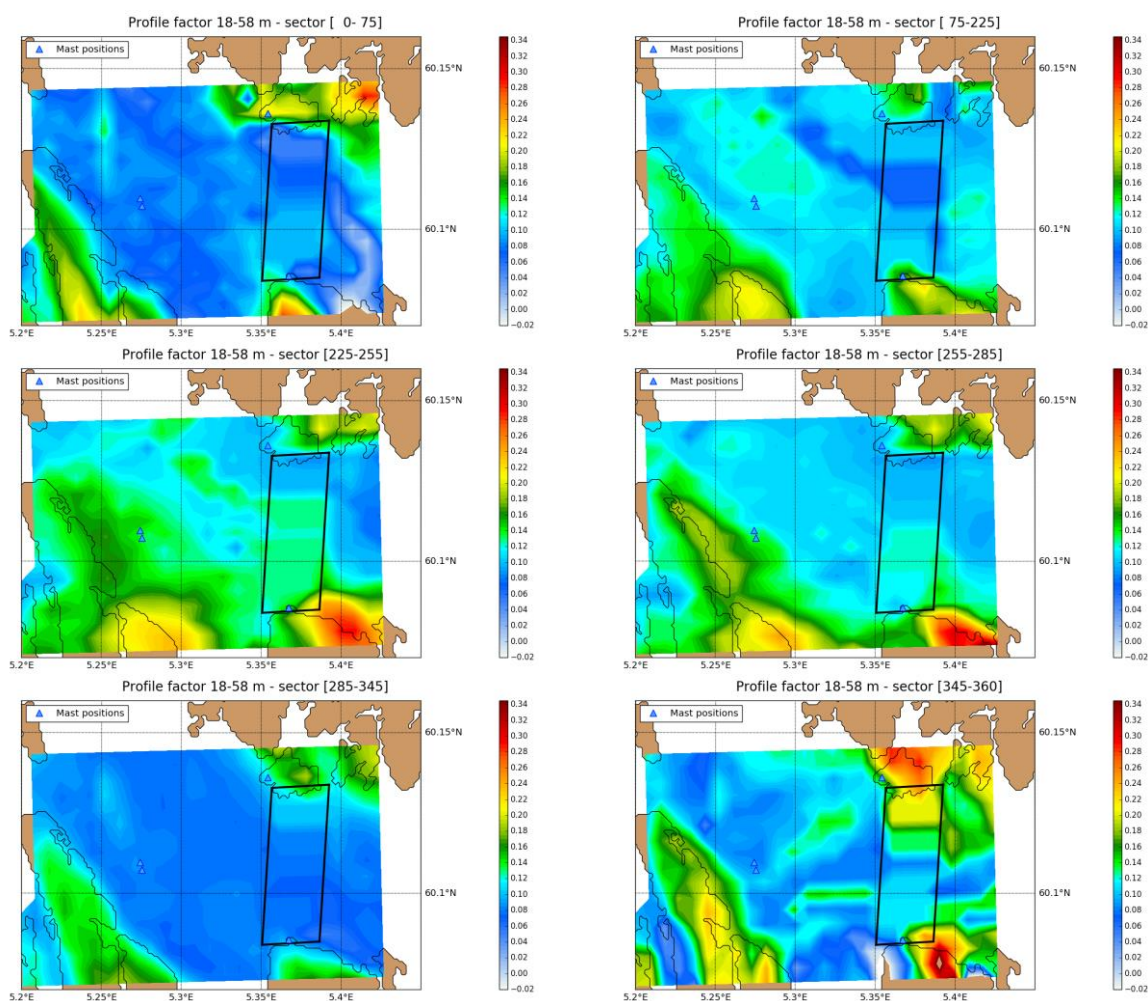


Figure B-1: Profile factors for WRF500m, between 18 m and 58 m. The fjord crossing  $\pm 1$  km is outlined as a black line.



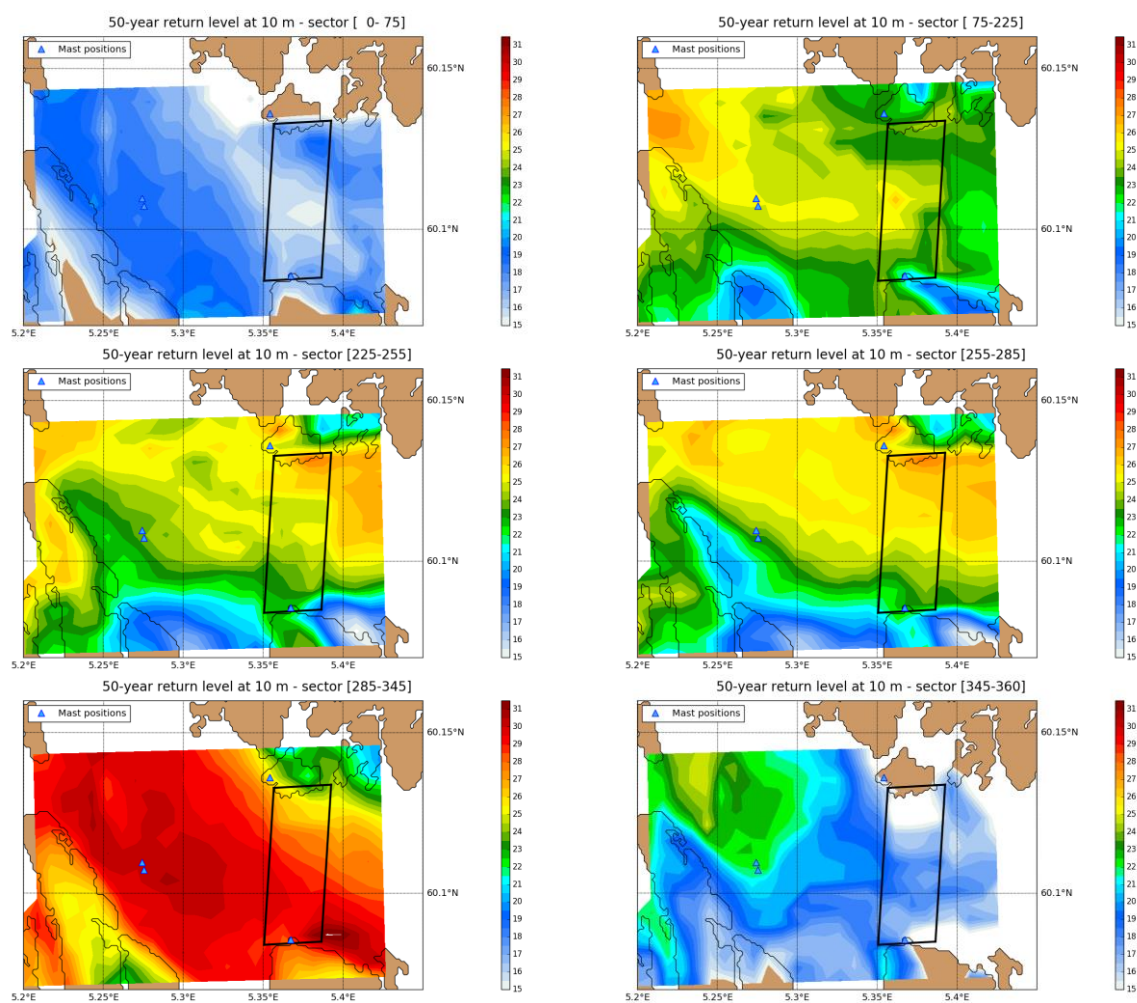


Figure B-2: 50-year return levels for hourly mean maximum, estimated at 10 m height using profile factors in Figure B-1. The fjord crossing  $\pm 1$  km is outlined as a black line.

## Appendix C - Additional tables

Table C-1: 50-year return levels for hourly mean wind [m/s] at 58 m.

Position	Wind direction						Max
	0-75	75-225	225-255	255-285	285-345	345-360	
North	21.1	28.1	31.6	31.5	32.1	21.7	32.1
North/middle	20.2	28.1	31.1	31.0	32.9	21.2	32.9
Middle	18.2	29.5	31.4	31.4	33.3	21.6	33.3
South/Middle	19.0	30.1	31.2	31.1	34.3	22.1	34.3
South	20.7	29.3	30.6	29.9	34.0	22.1	34.0

Table C-2: 50-year return levels for hourly mean wind [m/s] at 193 m.

Position	Wind direction						Max
	0-75	75-225	225-255	255-285	285-345	345-360	
North	24.3	33.6	36.4	36.3	36.3	28.4	36.4
North/middle	23.5	33.7	36.9	36.7	36.9	27.7	36.9
Middle	22.6	33.8	36.8	36.2	36.9	27.4	36.9
South/Middle	22.9	34.6	36.5	35.3	37.4	26.9	37.4
South	22.4	34.6	35.8	34.8	37.4	26.3	37.4

Table C-3: 50-year return levels for hourly maximum 10-minute average wind [m/s] at 10 m on bridge, estimated using detailed profile coefficients.

Position	Wind direction						Max
	0-75	75-225	225-255	255-285	285-345	345-360	
North	20.5	25.1	28.4	28.4	28.6	16.3	28.6
North/middle	19.0	26.7	26.5	27.8	30.5	18.0	30.5
Middle	16.8	28.2	27.0	27.1	31.1	20.0	31.1
South/Middle	17.1	27.1	26.7	26.9	32.2	20.1	32.2
South	18.7	26.0	26.2	25.9	31.9	19.3	31.9

## Conservative estimates

Table C-4: Conservative estimate of 50-year return levels for hourly mean wind [m/s] at 10 m, using profile coefficient 0.05 up to 58 m height.

Position	Wind direction						Max
	0-75	75-225	225-255	255-285	285-345	345-360	
North	19.3	25.7	28.9	28.9	29.4	19.9	29.4
North/middle	18.5	25.7	28.5	28.4	30.1	19.4	30.1
Middle	16.7	27.0	28.8	28.8	30.5	19.8	30.5
South/Middle	17.4	27.6	28.6	28.5	31.4	20.8	31.4
South	18.9	26.9	28.0	27.4	31.1	20.3	31.1

Table C-5: Conservative estimate of 50-year return levels for hourly mean wind [m/s] at 193 m, using profile coefficient 0.14, transferring the 58 m return levels (Table C-1) up to 193 m height. These results are the conservative version of Table C-2.

Position	Wind direction						Max
	0-75	75-225	225-255	255-285	285-345	345-360	
North	24.9	34.3	37.1	37.0	37.2	29.2	37.2
North/middle	24.2	35.2	37.6	37.5	38.5	28.3	38.5
Middle	23.6	35.5	38.1	37.3	38.8	28.2	38.8
South/Middle	24.0	36.7	38.3	37.1	39.7	28.5	39.7
South	23.9	36.3	37.8	36.8	39.3	27.8	39.3

## Appendix D - WRF

The Weather Research and Forecast (WRF) model is a state-of-the-art meso-scale numerical weather prediction system, aimed at both operational forecasting and atmospheric research needs. A description of the modelling system can be found at the home page <http://www.wrfmodel.org/>. The model version used in this work is v3.2.1 described in Skamarock et al. 2008<sup>1</sup>. Details about the modelling structure, numerical routines and physical packages available can be found in for example Klemp et al. (2000)<sup>2</sup> and Michalakes et al. (2001)<sup>3</sup>. The development of the WRF-model is supported by a strong scientific and administrative community in U.S.A. The number of users is large and it is growing rapidly. In addition the code is accessible for the public.

The most important input data are geographical data and meteorological data. The geographical data is from National Oceanic and Atmospheric Administration (NOAA). The data includes topography, surface data, albedo and vegetation. These parameters have large influence for the wind speed in the layers close to the ground. The ERA-Interim reanalysis data with approximately 0.7 degree resolution, available from the European Centre for Medium-Range Weather Forecasts (ECMWF) with 6 hours interval, is used as boundary data for the model. ERA-Interim is a reanalysis dataset resultant from the assimilation of all available observation data globally into a numerical weather prediction model in order to create a description of the state of the atmosphere on a uniform horizontal grid and at uniformly spaced time instants (00, 06, 12 and 18 UTC). The assimilation model incorporates data from several thousand ground based observation stations, vertical profiles from radiosondes, aircrafts, and satellites. See Berrisford et al. (2009)<sup>4</sup> and Dee et al. (2011)<sup>5</sup> for further description of the data. Surface roughness and landuse have been updated from Landmåteriets GSD database in Sweden and from the N50 series from Kartverket in Norway.

### WRF4km

The model setup used as reference for the long-term adjustment is shown in Figure D-1. The model has been set up with 4 km x 4 km horizontal resolution. The model is run with 32 layers in the vertical with four layers in the lower 200 m. We have used the Thompson microphysics scheme and the MYJ scheme for boundary layer mixing. The simulation outputs hourly data starting from 01.01.1979 and is updated continuously.



**Figure D-1: Model set up for the WRF reference simulations of Scandinavia.**

<sup>1</sup> Skamarock WC, Klemp JB, Dudhia J, Gill DO, Barker DM, Duda MG, Huang X-Y, Wang W. and Powers JG, 2008: A Description of the Advanced Research WRF Version 3, NCAR Technical Note NCAR/TN-475+STR, Boulder, June 2008

<sup>2</sup> Klemp JB., Skamarock WC. and Dudhia J., 2000: Conservative split-explicit time integration methods for the compressible non-hydrostatic equations (<http://www.wrf-model.org/>)

<sup>3</sup> Michalakes J., Chen S., Dudhia J., Hart L., Klemp J., Middlecoff J., and Skamarock W., 2001: Development of a Next Generation Regional Weather Research and Forecast Model. Developments in Teracomputing: Proceedings of the Ninth ECMWF Workshop on the Use of High Performance Computing in Meteorology. Eds. Walter Zwiefelhofer and Norbert Kreitz. World Scientific, Singapore.

<sup>4</sup> Berrisford P., Dee D., Fielding K., Fuentes M., Kållberg P., Kobayashi S. and Uppala S., 2009: The ERA-Interim archive. Version 1.0., ERA report series.

<sup>5</sup> Dee, D. P. and other authors, 2011: The ERA-Interim reanalysis: configuration and performance of the data assimilation system", Qart. J. R. Meteorol. Soc., 2011.

### WRF500m

The 500 m x 500 m simulation is run with the same WRF version as WRF4km. The vertical resolution is the same as for WRF4km, namely 32 levels, the two lowest levels are 18 m and 58 m. It is set up with four domains, having a resolution of 22.5 km x 22.5 km, 4.5 km x 4.5 km, 1.5 km x 1.5 km and 500 m x 500 m, respectively, as shown in Figure D-2.

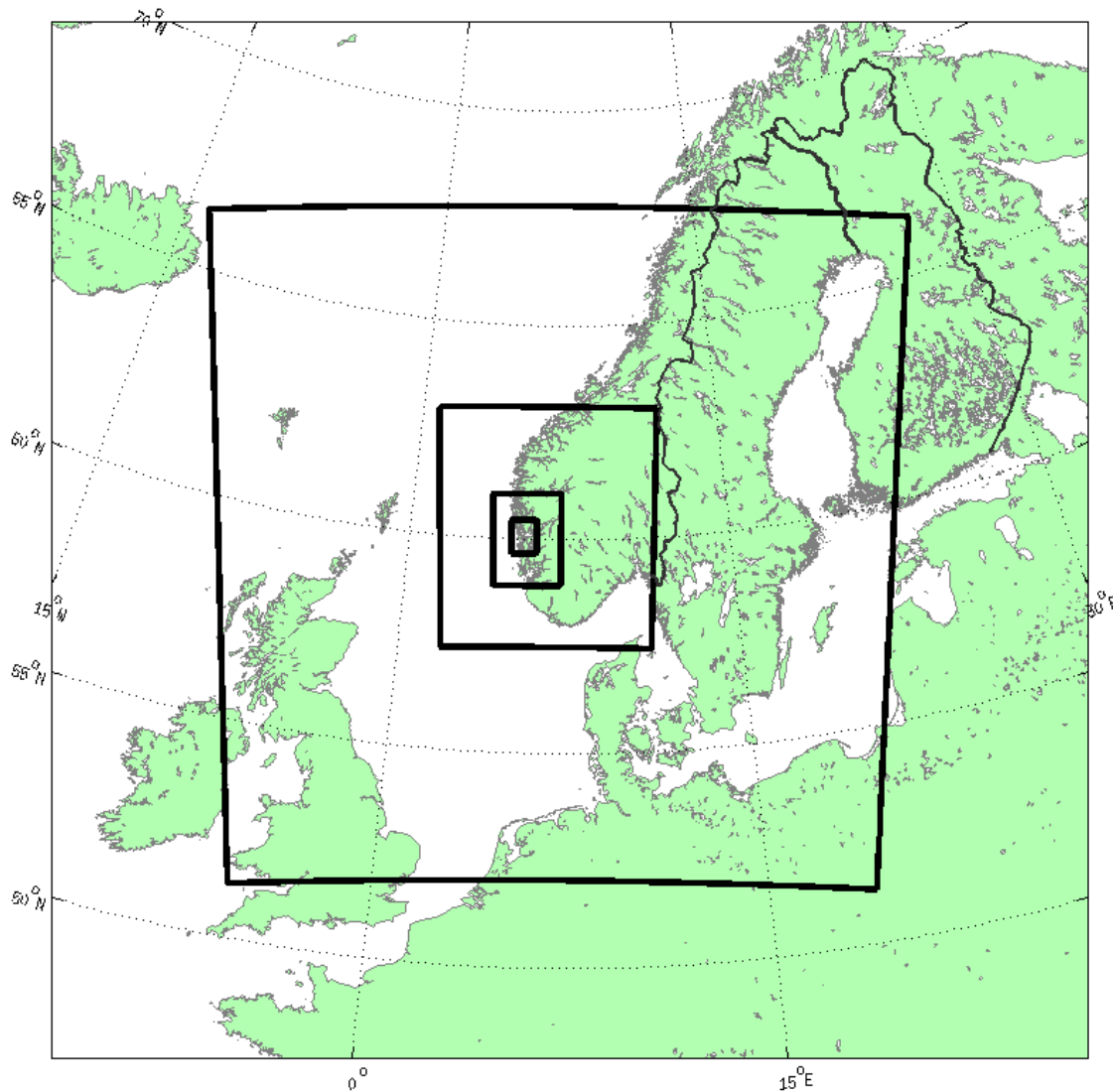
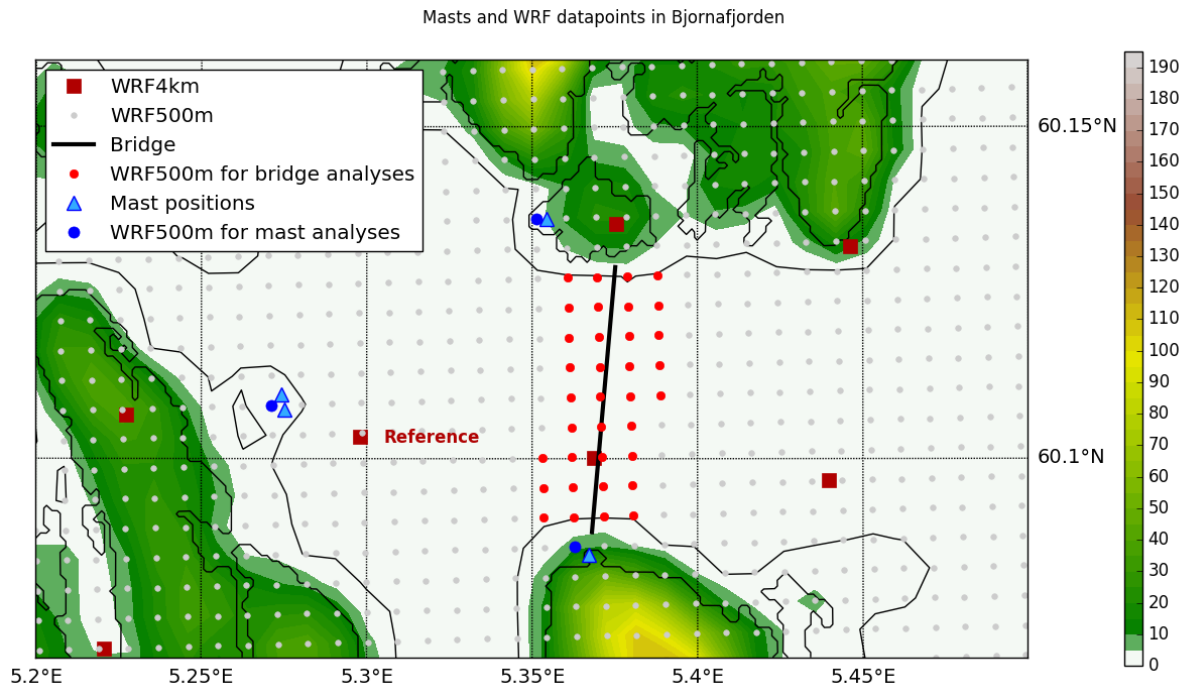


Figure D-2: Model set up for the WRF simulations of Bjørnafjorden.

The model grid points applied in the analyses are shown in Figure D-3. The long-term adjustment is carried out on all model grid points, using the same WRF4km reference, which is denoted Reference in Figure D-3. This reference point is selected because it is least subject to topography.



**Figure D-3: Model grid points used in the analyses. Also mast locations are shown. Blue WRF500m points are used in comparison with mast measurements. Red WRF500m points are used for estimating return levels at the fjord crossing. The only WRF4km data point used is denoted Reference.**